JOURNAL OF GEOPHYSICAL RESEARCH, VOL. 115, D13201, doi:10.1029/2009JD013276, 2010



# Carboxylic acids, sulfates, and organosulfates in processed continental organic aerosol over the southeast Pacific Ocean during VOCALS-REx 2008

L. N. Hawkins,[1] L. M. Russell,[1] D. S. Covert,[2] P. K. Quinn,[3] and T. S. Bates[3]

Received 25 September 2009; revised 8 February 2010; accepted 18 February 2010; published 2 July 2010.

[1] Submicron particles were collected on board the NOAA R/V *Ronald H. Brown* during the VAMOS Ocean-Cloud-Atmosphere-Land Study Regional Experiment (VOCALS-REx) in the southeast Pacific marine boundary layer in October and November 2008. The aerosol in this region was characterized by low numbers of particles (150–700 $cm^{-3}$) that were dominated by sulfate ions at concentrations of 0.9 ± 0.7 $\mu g\ m^{-3}$ and organic mass at 0.6 ± 0.4 $\mu g\ m^{-3}$, with no measurable nitrate and low ammonium ion concentrations. Measurements of submicron organic aerosol functional groups and trace elements show that continental outflow of anthropogenic emissions is the dominant source of organic mass (OM) to the southeast Pacific with an additional, smaller contribution of organic mass from primary marine sources. This continental source is supported by a correlation between OM and radon. Saturated aliphatic C-CH (alkane) composed 41 ± 27% of OM. Carboxylic acid COOH (32 ± 23% of OM) was observed in single particles internally mixed with ketonic carbonyl, carbonate, and potassium. Organosulfate $COSO_3$ (4 ± 8% of OM) was observed only during the periods of highest organic and sulfate concentrations and lowest ammonium concentrations, consistent with a sulfuric acid epoxide hydrolysis for proposed surrogate compounds (e.g., isoprene oxidation products) or reactive glyoxal uptake mechanisms from laboratory studies. This correlation suggests that in high-sulfate, low-ammonium conditions, the formation of organosulfate compounds in the atmosphere contributes a significant fraction of aerosol OM (up to 13% in continental air masses). Organic hydroxyl C-OH composed 20 ± 12% of OM and up to 50% of remote marine OM and was inversely correlated with radon indicating a marine source. A two-factor solution of positive matrix factorization (PMF) analysis resulted in one factor dominated by organic hydroxyl (>70% by mass) and one factor dominated by saturated aliphatic C-CH (alkane) and carboxylic acid (together, 90% by mass), identified as the marine and combustion factors, respectively. Measurements of particle concentrations in the study region compared with concentrations estimated from MODIS aerosol optical depth indicate that continental outflow results in MBL particle concentrations elevated up to 2 times the background level (less than 300 $cm^{-3}$) away from shore and up to 10 times the background level at the coast. The presence of both coastal fossil fuel combustion and marine sources of oxygenated organic aerosol results in little change in the oxygenated fraction and oxygen to carbon ratio (O/C) along the outflow of the region's dominant organic particle source.

**Citation:** Hawkins, L. N., L. M. Russell, D. S. Covert, P. K. Quinn, and T. S. Bates (2010), Carboxylic acids, sulfates, and organosulfates in processed continental organic aerosol over the southeast Pacific Ocean during VOCALS-REx 2008, *J. Geophys. Res.*, *115*, D13201, doi:10.1029/2009JD013276.

## 1. Background

[2] Aerosol particles in the marine boundary layer (MBL) are often mixtures of local primary (e.g., sea salt and organic compounds from sea spray), local secondary (e.g., sulfate from DMS oxidation), and transported primary and secondary emissions (e.g., organic carbon, elemental carbon, sulfate, nitrate, and ammonium) [*Quinn et al.*, 1996; *Maria et al.*, 2003; *Allan et al.*, 2004; *Quinn et al.*, 2006; *Hawkins et al.*, 2008; *Bates et al.*, 2008]. Relative contributions of the

[1] Scripps Institution of Oceanography, University of California at San Diego, La Jolla, California, USA.
[2] Department of Atmospheric Sciences, University of Washington, Seattle, Washington, USA.
[3] Pacific Marine Environmental Laboratory, NOAA, Seattle, Washington, USA.


0148-0227/10/2009JD013276

particle sources will determine the specific particle composition but organic compounds are almost always present and often compose a significant fraction of the total submicron mass [*Zhang et al.*, 2007]; the large number of organic compounds present in ambient aerosol, in combination with their wide variety of hygroscopic properties, makes solubility of multicomponent aerosols difficult to constrain using the available chemical information [*Ervens et al.*, 2005; *Prenni et al.*, 2007]. This constraint has resulted in the implementation of several methods to measure water uptake and solubility proxies including water soluble organic carbon (WSOC), optical hygroscopicity (f(RH)), and cloud condensation nuclei (CCN) concentration.

[3] Chemically based approaches to characterizing the properties of organic particle mixtures (in the absence of detailed compound quantification) have included identifying organic mass by the presence of heteroatoms (OM/OC) [*Russell*, 2003; *Russell et al.*, 2009a], the presence of functional groups [*Maria et al.*, 2002, 2003, 2004; *Gilardoni et al.*, 2007], or the atomic ratio of oxygen to carbon (O/C) [*DeCarlo et al.*, 2007; *Russell et al.*, 2009a]. These approaches rely on assumed relationships between these quantities and the mechanisms of their formation or the properties of the resulting organic mixtures.

[4] For example, O/C has been used to infer the degree of atmospheric processing or photochemical "age" of organic aerosols under the assumption that emitted organic aerosol becomes increasingly oxidized (increase in O/C) with age [*Maria et al.*, 2004; *Zhang et al.*, 2005a; *Johnson et al.*, 2005]. This trend is consistent with laboratory measurements of secondary organic aerosol (SOA) formation pathways [*Seinfeld et al.*, 2001; *Donahue et al.*, 2005; *Robinson et al.*, 2007] and field measurements of organic aerosol composition near organic particle sources [*Zhang et al.*, 2005a; *Russell et al.*, 2009a; *Liu et al.*, 2009]. However, in these cases, the majority of the aerosol was formed either from gas or particle phase hydrocarbon compounds in the absence of a primary source of oxygenated aerosol. This assumption is an oversimplification, for example, in the anthropogenically influenced marine atmosphere where primary emissions of oxygenated marine organic aerosol can mix with transported oxidized organic aerosol from continental sources [*Mochida et al.*, 2002; *Russell et al.*, 2010].

[5] Quantitative measurements of organic functional groups (measured either in bulk submicron or in single particles) provide additional, detailed information on organic composition beyond O/C or WSOC fraction. Fourier transform infrared (FTIR) measurements of carboxylic acid and organosulfate groups also provide estimates of the contribution of SOA to total OM, which is currently poorly understood [*Donahue et al.*, 2005; *Robinson et al.*, 2007]. Organosulfate groups in particular are a potentially large, yet currently rarely quantified, source of SOA owing to their ability to increase partitioning of semivolatile organic compounds from the gas phase to the particle phase [*Iinuma et al.*, 2007a, 2007b; *Surratt et al.*, 2007a, 2007b; *Iinuma et al.*, 2009; *Claeys et al.*, 2009].

[6] In this study we use measurements of particle concentrations, organic functional groups, elemental concentrations, and single particle composition to explore the composition, sources, and processes influencing submicron aerosol chemical composition in the MBL. We investigate organic composition from FTIR spectroscopy and from Quadrupole Aerosol Mass Spectrometry (Q-AMS) in order to improve our understanding of (1) the relative contributions of anthropogenic and marine sources to organic aerosol, (2) the oxidation of organic aerosols emitted from combustion sources, and (3) the significance and formation of organosulfate compounds in submicron aerosol. We also explore the significance and geographic distribution of continental outflow on the background MBL aerosol loading. The measurements used in this study were collected over a 42 day period aboard the NOAA R/V *Ronald H. Brown* (RHB) traveling near the western coasts of Peru and Chile using fixed temperature, relative humidity, and size-cut sampling protocols [*Bates et al.*, 2008].

## 2. Introduction

[7] The southeast Pacific MBL was the location of the VAMOS Ocean-Cloud-Atmosphere-Land Study Regional Experiment (VOCALS-REx) conducted in October and November 2008. Strong southeasterly surface winds north of 23°S in this region follow the coast lines of Chile and Peru and drive intense coastal upwelling, making the coastal surface waters significantly colder than those found at similar latitudes in other regions [*Garreaud and Muñoz*, 2005]. This cold surface water helps to sustain a large, uniform marine stratocumulus cloud deck present nearly year round [*Richter and Mechoso*, 2006]. The strong southeasterly surface winds also transport aerosol and aerosol precursor components (e.g., sulfate, $SO_2$, dust, and organic components) from cities such as Santiago, Chile, to the marine boundary layer increasing the background concentration of particles and potentially impacting cloud drop number, concentration, albedo and precipitation [*Artaxo et al.*, 1999; *Bretherton et al.*, 2004; *Huneeus et al.*, 2006]. A goal of the aerosol chemistry portion of the VOCALS-REx campaign was to characterize the composition, size, and variability of the submicron aerosol to improve understanding of the particle sources to the region and to better constrain the hygroscopic properties of the ambient aerosol. Radon (a decay product of rocks) has a 3.8 day half-life and was used to quantify the relative amount of continental influences on the sampled air masses. We have designated three air mass types based on radon concentrations and HYSPLIT back trajectories. Consistent with radon measurements, HYSPLIT back trajectories show air masses traveling from the south along the coast to the ship; air masses with back trajectories that had passed closer to land within 3 days of reaching the ship had higher radon concentrations.

## 3. Method

[8] Submicron particles were collected through an isokinetic sampling inlet located on the forward deck of the RHB approximately 18 meters above sea level (masl) [*Quinn et al.*, 2008; *Bates et al.*, 2008; *Russell et al.*, 2009a]. 37 mm Teflon filters (Pall Inc., 1 $\mu$m pore) for FTIR spectroscopic and X-Ray Fluorescence (XRF) analyses were located downstream of a 1 $\mu$m sharp-cut cyclone (SCC 2.229 PM1, BGI Inc.) in a humidity-controlled enclosure (60%) and were collected over 12 to 24 h (short samples)

with simultaneous 24 to 48 h duplicate samples. Sampling times were adjusted based on the organic mass concentration measured by the Aerodyne Quadrupole Aerosol Mass Spectrometer (Q-AMS). Long sampling times allowed improved signal-to-noise ratios for the low concentrations of the organic functional groups (<0.8 $\mu$g m$^{-3}$) in the relatively clean marine boundary layer (MBL).

[9] FTIR samples were kept at 0°C from the end of sample collection until FTIR spectroscopic analysis to reduce evaporative losses of organic compounds. For the earliest samples, this period was approximately 60 days. Duplicate back filters accompanied each sample filter for the entirety of the sampling process and were analyzed to quantify the adsorption of volatile compounds and other sources of contamination. These back filters showed negligible infrared absorption. FTIR absorbance spectra of each sample and back filter were measured nondestructively using a Bruker Tensor 27 spectrometer with RT-DLATGS detector [*Gilardoni et al.*, 2007] and were interpreted using a revised algorithm and calibration standards [*Russell et al.*, 2009a]. Quantified functional groups include saturated aliphatic C-CH (alkane), unsaturated aliphatic C=CH (alkene), aromatic C=CH, nonacidic organic hydroxyl C-OH (alcohol, including phenol), primary amine C-$NH_2$, nonacidic carbonyl C=O, carboxylic acid COOH, and organosulfate $COSO_3$ groups. Nonacidic carbonyl C=O, aromatic C=C-H, and unsaturated aliphatic C=C-H (alkene) groups were below detection limit in all samples and were omitted from the discussion presented here. Organosulfate groups absorb at 876 cm$^{-1}$ and have interference from $HSO_4^-$ and $CO_3^{2-}$ absorption. To quantify this interference, filters with detectable absorption at 876 cm$^{-1}$ were rinsed with 2 mL of hexane solvent, which removes the organosulfate-containing compounds but not bisulfate or carbonate [*Maria et al.*, 2003; *Gilardoni et al.*, 2007]. Concentrations of organosulfate were determined from the peak area removed by the hexane rinse (which resulted in complete removal of the absorbance at 876 cm$^{-1}$) and an ethylsulfate calibration standard. The sum of all measured organic functional groups is used to determine organic mass (OM) concentration for each filter period. X-ray fluorescence on the Teflon filters was completed by Chester Labnet (Tigard, Oregon) and provided concentrations of Na and heavier elements [*Maria et al.*, 2003; *Gilardoni et al.*, 2007; *Russell et al.*, 2009a].

[10] The Aerodyne Quadrupole Aerosol Mass Spectrometer (Q-AMS) measures bulk nonrefractory submicron aerosol chemical composition and component-specific size distributions in real time. Only a brief description is provided here; more detailed information on the Q-AMS is given by *Jayne et al.* [2000] and *Jimenez et al.* [2003]. The instrument consists of an aerodynamic lens followed by a rotating chopper. This time-of-flight (ToF) region is followed by a 600°C vaporizer and electron impact ionizer. From there the sample is analyzed using a quadrupole mass spectrometer with 1 amu resolution. Quantified components include $SO_4^{2-}$, $NO_3^-$, $NH_4^+$, and organic mass. Collocated multistage impactors were used to collect inorganic samples for extraction and ionic analysis (761 Compact IC, Metrohm) [*Quinn et al.*, 2006, 2008; *Bates et al.*, 2008]. $SO_4^{2-}$ and $NH_4^+$ from ion chromatography (IC) analysis of the impactor samples were used to derive the collection efficiency of the AMS for the inorganic ions [*Quinn et al.*, 2006]. The project average shows good correlation for sulfate (AMS versus IC slope = 1.09, r = 0.94) and ammonium (AMS versus IC slope = 0.85, r = 0.9) between the two methods and a collection efficiency (CE) of 1 is applied to the inorganic AMS measurements. The CE of organic mass was lower than 1 based on the FTIR/AMS comparison of OM as described in section 4.3. Collocated measurements of condensation nuclei (CN) concentration for particle diameters greater than 13 nm were collected using a TSI 3010 condensation particle counter (CPC) on the shared inlet at 1 min resolution. Particle number–size distribution was measured on a 5 min time basis by a combination of mobility and aerodynamic particle sizing from 20 nm to 10 $\mu$m diameter [*Bates et al.*, 2008].

[11] From the same isokinetic inlet, single particles were collected by impaction onto silicon nitride windows ($Si_3N_4$, Silson Ltd, Northampton, England) for 30 min periods (Streaker, PIXE International Corp., Tallahassee, Florida). The windows were kept at 0°C prior to analysis by Scanning Transmission X-ray Microscopy-Near Edge X-ray Fine Structure (STXM-NEXAFS) at the Advanced Light Source at Lawrence Berkeley National Laboratory in Berkeley, California [*Takahama et al.*, 2007, 2010]. Particle morphology (e.g., spherical, irregular, or cubic) and mixture type (e.g., sea salt–organic, dust-organic, or combustion) can be determined from single particle images and optical density spectra of the carbon K edge (between 278 and 305 eV). Mixture type is determined from STXM-NEXAFS spectra based on relative amounts of components (i.e., alkane, alkene, carboxylic carbonyl, ketonic carbonyl, carbonate, and potassium).

## 4. Results

### 4.1. Regional Extent of Continental Outflow to the MBL

[12] Remote sensing measurements of cloud drop radius analyzed by *Bretherton et al.* [2004] and *Huneeus et al.* [2006] have indicated that the large pollution sources, especially copper smelters, along the Peruvian and Chilean coasts could impact particle concentrations, cloud properties, and cloud albedo in the southeast Pacific MBL by significantly increasing particle concentrations above background levels, resulting in longitudinal gradients in particle concentration and cloud drop radii. One of the goals of the VOCALS-REx study was to quantify the extent of this continental outflow on the stratocumulus-topped boundary layer near 20°S. Defining a particle concentration for the "clean" marine atmosphere is not straightforward, as background concentrations are regionally and temporally variable. However, a survey of previous studies (Figure 1a) suggests that particle concentrations (CN) between 300 and 500 cm$^{-3}$ are a reasonable upper limit for the clean MBL [*Pirjola et al.*, 2000; *Bates et al.*, 2000; *O'Dowd et al.*, 2001; *Twohy et al.*, 2005; *Andreae*, 2009]. Particle concentrations in the MBL defined as "polluted" in the same studies range from greater than 400 cm$^{-3}$ to greater than 1500 cm$^{-3}$. VOCALS-REx average CN concentration was 350 ± 135 cm$^{-3}$, corresponding to a clean to moderately polluted MBL. Shipboard observations are limited to the cruise track and sampling times, so obtaining a regional

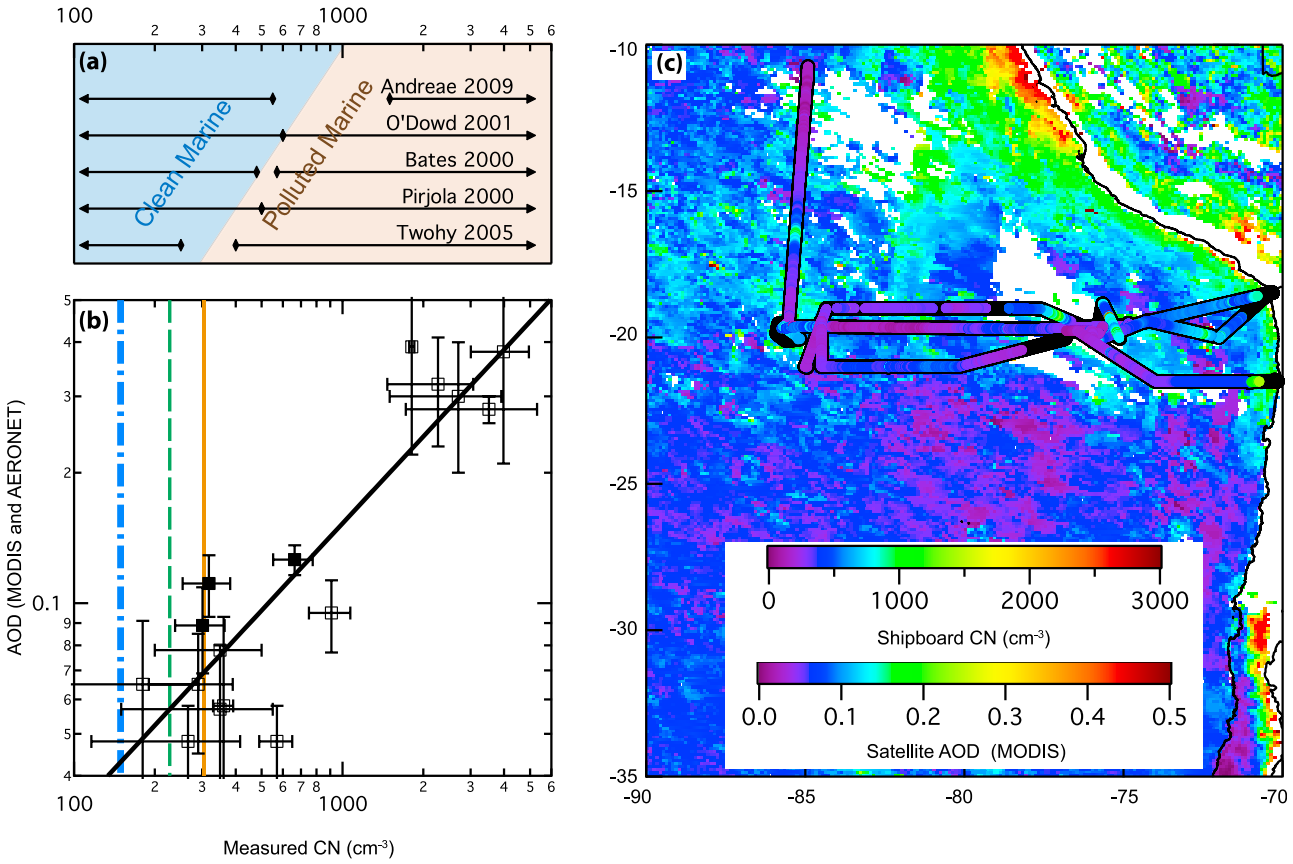


**Figure 1.** (a) Particle concentrations (and ranges of concentrations) classified as "clean marine" and "polluted marine" in previous studies. (b) Satellite-derived AOD from MODIS (this work, solid squares) and AERONET (*Andreae* [2009], open squares) compared with CN measurements. In all cases, error bars represent 1 standard deviation on the mean. The best fit line ($AOD = 0.0017 \times CN^{0.66}$) includes both MODIS and AERONET measurements. Blue dash-dotted, green dashed, and tan solid vertical lines mark the average CN concentration during MAM, XAM, and CAM periods, respectively. (c) Average MODIS AOD for October and November 2008 for study region. White regions (missing data) were cloudy during both October and November. Cruise track of the NOAA R/V *Ronald H. Brown* is shown in black. Shipboard CN measurements are overlaid on the cruise track.

picture of continental outflow from in situ measurements is difficult.

[13] To address this issue, measurements of aerosol optical depth (AOD) from the MODerate resolution Imaging Spectroradiometer (MODIS) aboard NASA's Terra spacecraft were compared with filter-averaged CN concentrations when the satellite passed over the cruise track during clear-sky conditions. AOD was averaged over the entire latitude and longitude range traveled during the filter period. Due to the narrow satellite path and frequently cloudy skies, only three filters met the conditions for quantitative comparison. Measurements of $AOD_{500}$ from the ground-based AErosol RObotic NETwork (AERONET) and collocated measurements of CN concentration compiled by *Andreae* [2009] for clean and polluted marine environments were added to the comparison. Figure 1b shows the relationship between AOD and CN concentration for VOCALS-REx and previous studies in marine environments. MODIS AOD is slightly higher than AERONET AOD for similar aerosol loading though differences within the AERONET measurements for similar aerosol loadings are equally as large. Validation studies suggest that the two measurements agree within 2% when measurements are compared for the same wavelengths [*Remer et al.*, 2002].

[14] Figure 1c shows the average MODIS AOD for October and November 2008 during clear-sky conditions. South of 23°S, AOD is largely below 0.1, corresponding to CN concentrations less than 300 $cm^{-3}$ based on the comparison in Figure 1b. This horizontal band of low AOD is expected from westerly surface winds that increase in intensity from about 23°S to 30°S and bring relatively clean marine air to the southeast Pacific. North of 23°S, surface winds are generally easterly [*Bretherton et al.*, 2004] bringing polluted air masses from the Chilean coast west to the study region. Shipboard CN measurements have been converted to AOD using the best fit line for all points in Figure 1b. From only shipboard measurements, the latitudinal trend in AOD is not visible. A weak longitudinal trend is present, but the sharp decrease in AOD with distance from the coast is masked by patchy areas of intermediate aerosol loading. Because of the surface winds, the steep longitudinal gradient in particle concentration is super-

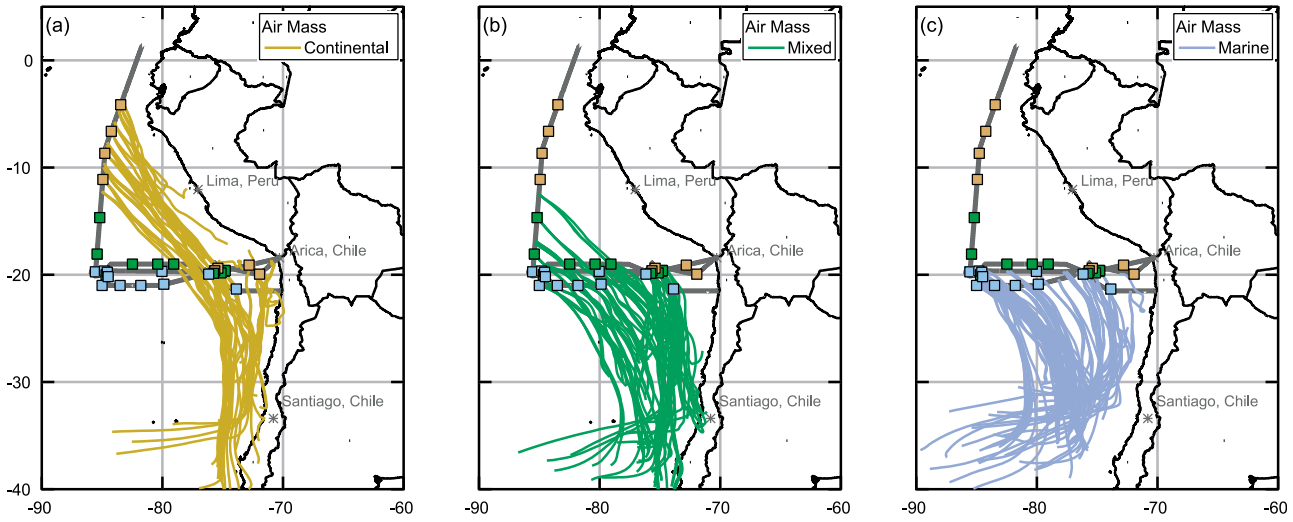


**Figure 2.** Track of the NOAA R/V *Ronald H. Brown* during VOCALS-REx from 21 October to 30 November 2008 and average location of each filter, marked by colored squares. Squares are colored by air mass assignment determined from average radon concentration. Nine 3 day HYSPLIT back trajectories (beginning, middle, and end of filter period at 50 m, 100 m, and 500 masl) are shown for (a) continental (CAM), (b) mixed (XAM), and (c) marine air masses (MAM).

imposed on the large-scale latitudinal trend. Near shore AOD ranged from 0.15 to 0.4 corresponding roughly to CN concentrations between 600 and 4000 $cm^{-3}$, with the highest AOD occurring within the first several hundred kilometers from the coast. AOD values from 0.1 to 0.15 (representing 300 to 600 $cm^{-3}$), corresponding to a doubling of background particle concentration, were observed at distances even greater than 1000 km from the nearest coastline in the region north of 23°S. Therefore, the outflow of continental emissions has only a minor, near-shore influence in the region south of 23°S, while the region north of 23°S appears to have particle concentrations significantly elevated above background levels, which would result in greater potential direct and indirect aerosol effects in, and to the north of, the VOCALS-REx study region. This finding supports the proposed hypothesis that continental outflow from the South American coast has a significant impact on ambient aerosol concentrations.

[15] For in situ measurements, radon concentrations were used to categorize VOCALS-REx air masses as "continental" air masses (CAM), "mixed" air masses (XAM), and "marine" air masses (MAM). Based on calibrations, the lower limit of detectable radon for the project was 200 mBq $m^{-3}$. However, an increase in the background concentration of radon between the first and second calibration periods and subsequent adjustment to the concentrations means that different radon concentration limits were needed for each leg to assign air mass categories. For Leg 1, MAM periods were defined by radon less than 250 mBq $m^{-3}$, CAM periods were defined by radon greater than 350 mBq $m^{-3}$, and XAM periods were defined between the two concentrations. For Leg 2, MAM periods were defined by radon less than 150 mBq $m^{-3}$, CAM periods were defined by radon greater than 300 mBq $m^{-3}$, and XAM periods were defined between the two concentrations. This assignment is a simplification to highlight similarities and differences among the samples and not to imply that only one type of particle was measured at a given time. In Figure 1b, colored vertical lines mark the average CN concentration during MAM, XAM, and CAM periods. For each filter, HYSPLIT back trajectories were calculated for the start, middle, and end of the sampling period at 50 masl, 100 masl, and 500 masl (Figure 2) and are shown colored by air mass category. For most of the cruise, air masses traveled north, northeast, or east while south of 30°S latitude and then turned northwest, generally following the coastline. Radon measurements are consistent with HYSPLIT back trajectories; samples measured near the coast had higher radon (up to 1000 mBq $m^{-3}$) than those measured near 85°W latitude (less than 300 mBq $m^{-3}$).

### 4.2. Cluster Analysis of FTIR Spectra

[16] Hierarchical Ward cluster analysis [*Ward*, 1963] was used to separate the 31 sample FTIR spectra into three clusters (Figure 3). For the cluster analysis, only absorbance between 4000 $cm^{-1}$ and 1500 $cm^{-1}$ was considered due to Teflon interference below 1300 $cm^{-1}$ and the absence of quantified groups other than organosulfate below 1500 $cm^{-1}$. Using more than three clusters resulted in clusters with only 3 spectra, which were considered too small to be meaningful. Cluster 1 has the highest carboxylic acid and alkane fractions and a significantly lower organic hydroxyl fraction than the other clusters. Cluster 2 has twice the fraction of organic hydroxyl groups of Cluster 1 and less carboxylic acid and alkane groups. Cluster 3 has only slightly higher organic hydroxyl and lower alkane groups than Cluster 2 but includes three sample spectra all observed at the cruise location farthest from land and one sample with over 40% organic hydroxyl groups.

[17] Figure 3d shows the fraction of sample spectra observed during each of the three air mass periods. Cluster 1 was observed in all three air mass types but was the dominant spectra type observed during CAM periods (63%) and was only observed in 17% of MAM periods indicating that the average composition of Cluster 1 represents the com-

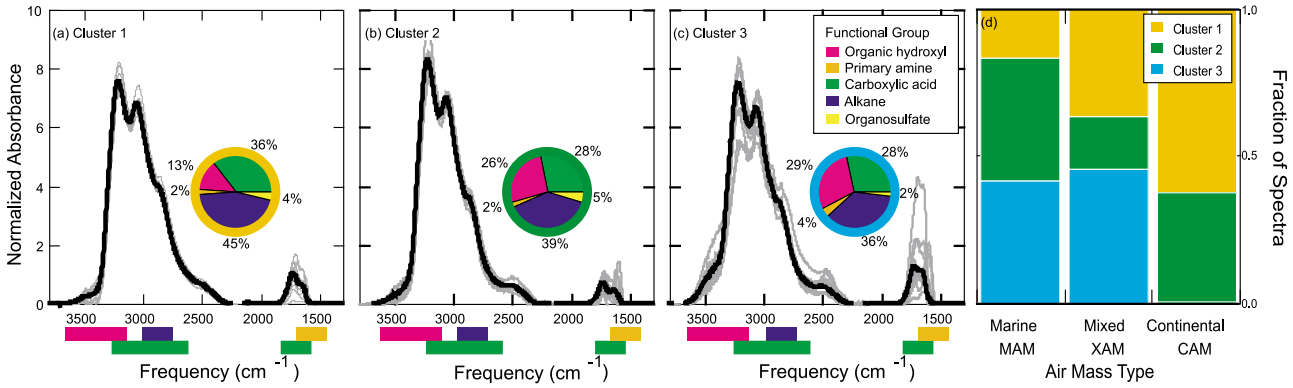


**Figure 3.** (a, b, and c) Ward cluster analysis on the 31 normalized sample spectra produced three clusters. Average spectra of each cluster are shown in black. Pie charts show the average functional group composition of each cluster. Colored bars shown along the *x* axis correspond to functional groups in the legend and indicate approximate absorbance region of each functional group with the exception of organosulfate, which is not included in the cluster analysis but is shown on the pie charts. (d) Fraction of sample spectra from each cluster for MAM, XAM, and CAM.

position of processed continental organic aerosol. Cluster 3 was observed only during XAM (45%) and MAM (42%) periods, indicating that the higher organic hydroxyl fraction was related to a larger contribution from a marine organic source.

### 4.3. Organic, Inorganic, and Elemental Components

[18] Figure 4 shows FTIR organic functional groups, AMS sulfate, ammonium, nitrate, and organic components. OM fraction from marine and combustion factors identified from PMF analysis for October and November 2008 are also shown (described in detail in section 4.4). The variation in continental influence (radon) correlates with FTIR OM and AMS sulfate over the campaign. The sum of the organic functional groups defines total organic mass from FTIR. After 18 November the AMS was operated in the full scan mode (m/z range 0–300) with the particle beam permanently unblocked due to chopper motor malfunction. The background gas signal was obtained by closing the valve periodically, so sulfate concentrations after 18 November may have a higher uncertainty than measurements collected during normal operation, though baseline sulfate measured during the valve closed periods showed no change from baseline sulfate measured during normal operation. Organics, ammonium, and nitrate mass spectra overlap with air mass spectra and could not be estimated from the modified "closed" signal. Colored bars across the top axis show CAM, XAM, and MAM periods; total OM and sulfate were highest during CAM periods and lowest during MAM periods. Average concentrations of organic, inorganic, and elemental components for the campaign and CAM, XAM, and MAM periods are shown in Table 1. Sulfate was the dominant component of the submicron mass with an average of 0.93 ± 0.67 $\mu$g m$^{-3}$ and ranged from 0.67 ± 0.33 $\mu$g m$^{-3}$ in MAM to 1.4 ± 1.0 $\mu$g m$^{-3}$ in CAM. FTIR OM was between 0.18 and 1.9 $\mu$g m$^{-3}$ with a project average of 0.59 ± 0.37 $\mu$g m$^{-3}$. FTIR OM was only 0.4 ± 0.17 $\mu$g m$^{-3}$ in MAM compared with 1.0 ± 0.5 $\mu$g m$^{-3}$ in CAM. The average composition of the organic mass was 41 ± 27% alkane, 32 ± 23% carboxylic acid, 20 ± 12% organic hydroxyl, 3 ± 2% primary amine, and 4 ± 8% organosulfate. Average carboxylic acid fraction showed a small decrease from CAM to MAM while average organic hydroxyl fraction increased from 16% to 22%. O/C and OM/OC average ratios for the entire campaign were 0.62 ± 0.12 and 2.0 ± 0.19, respectively, and showed little change over the three air mass types. Elements above detection limit in greater than 20% of samples include S, Sn, V, Fe, K, Br, Ca, and Ni; other elements measured by XRF were below detection limit in more than 80% of the samples and are not included in chemical comparisons. Concentrations of all reported elements show a decrease from CAM to MAM, with intermediate values reported for XAM, consistent with the air mass classification. Submicron Na and Cl from ion chromatography were above detection limit in most samples and composed 9 ± 6% of $PM_1$ on average.

[19] Figure 5 shows the relationship of OM, sulfate, XRF elements, carboxylic acid fraction, organic hydroxyl fraction, FTIR O/C, and AMS m/z 44 fraction with radon. FTIR OM, dust and metals, and carboxylic acid fraction have mild correlations with radon (r = 0.60, 0.74, and 0.54, respectively). AMS sulfate has a weak positive correlation to radon (0.43), possibly because the Chilean copper smelters have a stronger influence on sulfate concentration near the southern part of the cruise track while radon was higher near the northern part of the cruise track (along the coast of Peru). The organic hydroxyl fraction shows no correlation to radon (r = −0.23). Alkane fraction (not shown in Figure 5) does not show a trend with radon despite likely having a continental source and being removed by oxidation during atmospheric processing. This observation suggests that there were contributions from both continental and marine sources to alkane groups.

[20] FTIR O/C and AMS m/z 44 fraction of OM are shown in the first and second plot of Figure 5. FTIR O/C is calculated from the total number of oxygen atoms from oxygen-containing functional groups normalized by the total number of carbon atoms from all groups [*Gilardoni et al.*, 2007; *Russell et al.*, 2009a]. AMS O/C is estimated from the ratio of m/z 44 fragment to AMS OM, which has shown a consistent relationship with atomic O/C from Elemental Analysis (EA) for both laboratory and field measurements [*Aiken et al.*, 2008]. The accuracy of reproducing atomic

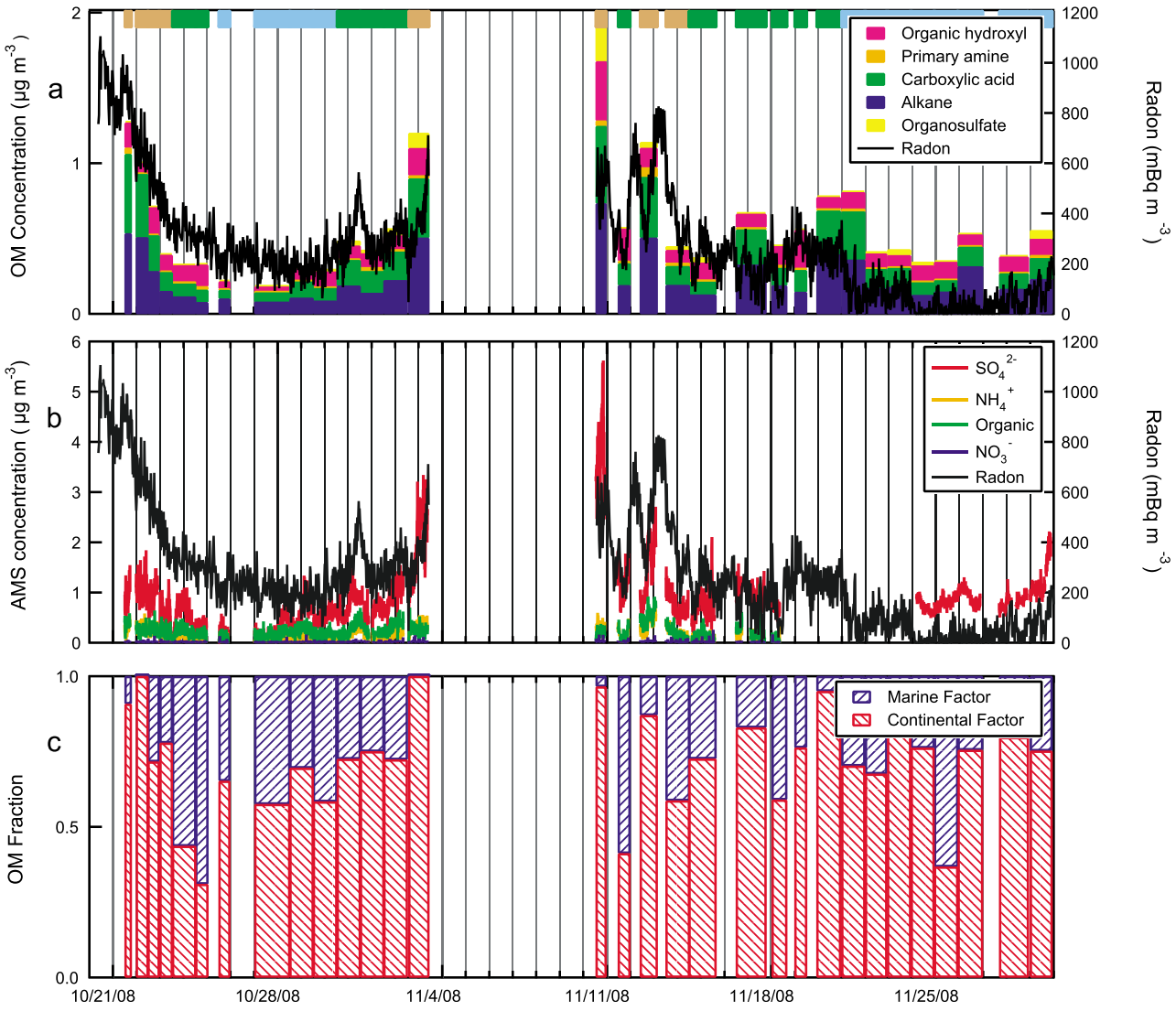


**Figure 4.** Time series of (a) FTIR functional groups, (b) AMS inorganic and organic components, and (c) fraction of OM from marine and combustion PMF factors. Colors across the top of Figure 4a indicate air masses: CAM (tan), XAM (green), and MAM (blue). AMS organics, nitrate, and ammonium are not available after 18 November because of instrument malfunction. AMS sulfate has been estimated from the MS open mode and the valve closed signal. Radon is a proxy for continental influence.

O/C from EA varies with organic compounds and is based on the fragmentation of organic acid groups which are assumed to be present in proportion to other oxygen-containing organic functional groups, including organic hydroxyl groups [*Aiken et al.*, 2007]. The m/z 44 fraction of AMS OM, which is reported to have a linear relationship with atomic O/C [*Aiken et al.*, 2007] correlates with radon (r = 0.56) while FTIR O/C shows no clear trend with radon reflecting the composition of the organic mass based on a mixture of both carboxylic acid and other oxygenated organic functional groups (discussed in detail in section 5.2).

### 4.4. Comparisons of FTIR and AMS Organic and Sulfate Concentrations

[21] FTIR OM was correlated with AMS OM (r = 0.7) and was higher than AMS OM by a factor of 2.4 on average (Figure 6). In previous field measurements, the two methods have been within 20% of each other, which is within the 20–30% uncertainty associated with both measurements [*Gilardoni et al.*, 2007, 2009; *Russell et al.*, 2009a]. Adsorption of organic gases onto the filters was eliminated as a possible reason for the discrepancy because the back filters showed negligible OM and the discrepancy in OM was independent of sampling duration and showed no diurnal dependence. A portion of this difference can be explained by organosulfate $COSO_3$ groups. In AMS mass spectra and the fragmentation table used to assign mass fragments to particular components, only the carbon-containing fragment of the organosulfate would be attributed to organic mass. The sulfate fragment typically would be attributed to inorganic sulfate leading to a smaller organic mass measured by AMS than by FTIR when organosulfate groups are present.

**Table 1.** Mean and Standard Deviation of Measured OM, Organic Functional Group, O/C, m/z 44 Fraction, and Elemental Concentrations for VOCALS-REx and for Periods Defined as CAM, XAM, and MAM

| | VOCALS-REx | CAM | XAM | MAM |
|---|---|---|---|---|
| Distance to Coast (km) | 580 ± 230 | 370 ± 160 | 520 ± 240 | 670 ± 180 |
| Average Radon (mBq $m^{-3}$) | 270 ± 200 | 530 ± 180 | 380 ± 180 | 110 ± 80 |
| CN < 80 nm ($cm^{-3}$) | 122 ± 90 | 100 ± 65 | 102 ± 55 | 154 ± 124 |
| CN > 80 nm ($cm^{-3}$) | 197 ± 102 | 305 ± 130 | 227 ± 114 | 149 ± 55 |
| Average modal $D_p$ (nm)[a] | 340 ± 20 | 340 ± 16 | 340 ± 23 | 360 ± 19 |
| FTIR OM ($\mu g\ m^{-3}$) | 0.59 ± 0.37 | 1.0 ± 0.5 | 0.71 ± 0.42 | 0.4 ± 0.17 |
| AMS OM ($\mu g\ m^{-3}$) | 0.23 ± 0.10 | 0.29 ± 0.11 | 0.24 ± 0.10 | 0.17 ± 0.10 |
| AMS $SO_4^{2-}$ ($\mu g\ m^{-3}$) | 0.93 ± 0.67 | 1.4 ± 1.0 | 1.1 ± 0.8 | 0.67 ± 0.33 |
| FTIR Organic Functional Groups ($\mu g\ m^{-3}$) | | | | |
| Alkane | 0.24 ± 0.16 (41%) | 0.43 ± 0.20 (43%) | 0.30 ± 0.19 (40%) | 0.17 ± 0.09 (43%) |
| Carboxylic acid | 0.19 ± 0.13 (32%) | 0.34 ± 0.16 (34%) | 0.23 ± 0.15 (33%) | 0.11 ± 0.069 (29%) |
| Organic hydroxyl | 0.12 ± 0.068 (20%) | 0.16 ± 0.10 (16%) | 0.14 ± 0.078 (20%) | 0.088 ± 0.025 (22%) |
| Amine | 0.015 ± 0.014 (3%) | 0.023 ± 0.023 (2%) | 0.019 ± 0.015 (3%) | 0.0089 ± 0.0068 (2%) |
| Organosulfate | 0.023 ± 0.047 (4%) | 0.051 ± 0.085 (5%) | 0.029 ± 0.058 (4%) | 0.015 ± 0.019 (4%) |
| FTIR O/C (atomic) | 0.62 ± 0.12 | 0.58 ± 0.073 | 0.63 ± 0.13 | 0.59 ± 0.13 |
| FTIR OM/OC (mass) | 2.0 ± 0.19 | 2.0 ± 0.11 | 2.1 ± 0.19 | 2.0 ± 0.20 |
| AMS m/z 44 fraction (mass) | 0.085 ± 0.057 | 0.14 ± 0.028 | 0.099 ± 0.052 | 0.023 ± 0.035 |
| XRF Elements (ng $m^{-3}$ unless specified) | | | | |
| S ($\mu g\ m^{-3}$) | 0.23 ± 0.15 | 0.42 ± 0.19 | 0.29 ± 0.17 | 0.15 ± 0.046 |
| V | 0.29 ± 0.18 | 0.43 ± 0.17 | 0.34 ± 0.172 | 0.12 ± 0.15 |
| Br | 0.39 ± 0.18 | 0.59 ± 0.25 | 0.43 ± 0.21 | 0.30 ± 0.083 |
| Sn | 5.9 ± 4.4 | 9.6 ± 6.5 | 7.8 ± 4.9 | 3.4 ± 1.5 |
| Ni | 1.1 ± 0.81 | 1.2 ± 0.82 | 1.3 ± 0.86 | 0.59 ± 0.13 |
| K | 7.0 ± 7.7 | 15 ± 12 | 9.4 ± 8.9 | 3.5 ± 3.0 |
| Fe | 1.3 ± 1.4 | 2.0 ± 1.8 | 1.6 ± 1.5 | 0.52 ± 0.18 |
| Ca | 1.7 ± 0.96 | 2.6 ± 1.1 | 2.0 ± 0.94 | 0.93 ± 0.42 |

[a]Average modal electrical mobility diameter of the accumulation mode volume-size distribution.

However, the organosulfate contribution can only explain a small fraction of the observed difference in OM between the two methods because sulfate from organosulfate groups composes only 0% to 12% of OM.

[22] Another possible explanation for the discrepancy is an AMS OM collection efficiency (CE) less than the 100% measured for sulfate. Laboratory and field measurements have shown that solid particles have a much lower CE than liquid particles [*Matthew et al.*, 2008] due to particles bouncing off the vaporizer before volatilization. For example, drying ammonium sulfate below its efflorescence relative humidity can reduce the CE of submicron particles from 100% to as low as 20% [*Alfarra et al.*, 2004; *Allan et al.*, 2004; *Matthew et al.*, 2008]. Ambient organic compounds are mostly present as liquids and generally have 100% CE [*Alfarra et al.*, 2004; *Zhang et al.*, 2005b] when they are not mixed with other components. The CE of organic components in organic and sulfate mixtures can be approximated to the CE of sulfate, generally measured independently [*Jimenez et al.*, 2003; *Drewnick et al.*, 2003; *Bates et al.*, 2005; *Quinn et al.*, 2006]. However, the collection efficiency of organic mass may be lowered if the organic compounds are present on refractory particles with very low collection efficiencies, especially if the ratio of organic mass to refractory material is low. The CE of refractory material is not measurable since the AMS can only measure species that volatilize at the set operating temperature (600°C). In this case, only an independent measure of OM can provide an accurate determination of organic CE, similar to the correction applied to AMS sulfate by collocated, time-integrated ion chromatography.

[23] The difference in OM between FTIR and AMS is correlated (r = 0.8) with the concentration of dust elements (nss-K, nss-Ca, Al, Si, Fe, and Ti) measured by XRF of Teflon filters (Figure 6, inset). Aluminum and silicon are included here for above detection limit samples although they were not above detection in more than 20% of the samples and they are not included in Table 1. This relationship is consistent with the hypothesis that the reduced CE of AMS organic mass was caused by particles containing organic and dust components bouncing off the AMS vaporizer. Some of the difference in measured OM could also be attributed to organic components that were present on particles small enough to be sampled by FTIR but large enough to have less than 100% transmission into the AMS particle beam. Further, organic single particles identified with STXM-NEXAFS that were internally mixed with carbonate and potassium, corresponding to type "f" spectra (dust) from *Takahama et al.* [2007], represent 47 of the 96 submicron single particles analyzed. Other identified types include secondary (type "a"), biomass (types "i" and "j"), and combustion (an umbrella class including six particle types) (Figure 7a). In previous studies, dust type single particles have composed less than 20% of the measured particles [*Takahama et al.*, 2007]. Figure 7b shows the average optical density spectrum of VOCALS organic dust particles, with strong absorbances from carboxylic carbonyl, carbonate, and potassium. Using an algorithm developed by *Takahama et al.* [2010], the organic mass fraction of some particles identified as organic and dust mixtures was estimated to be 0.34 ± 0.24 on average. The uncertainty associated with the estimated organic mass fraction depends on the homogeneity of the single particle mixture and varies widely over the analyzed particles, but it is clear that the particles have significant dust fractions that may make them more susceptible to phase-dependent particle bounce in the

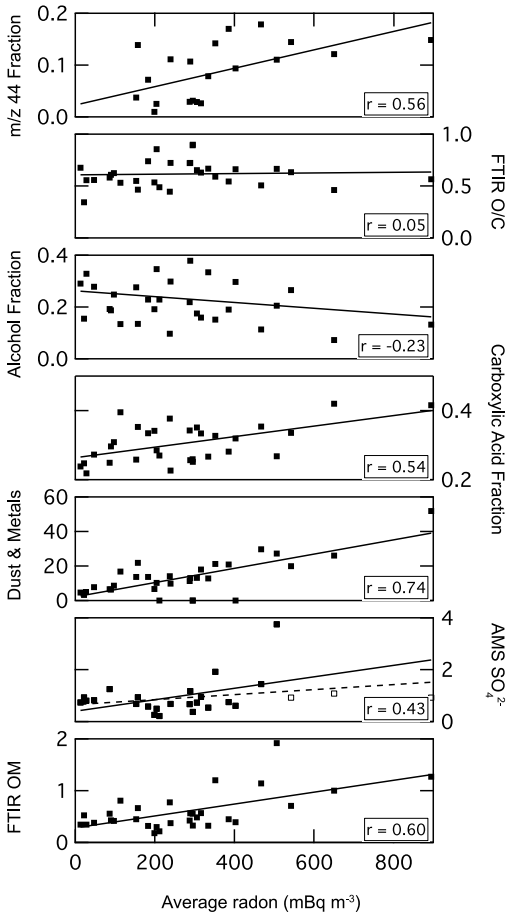


**Figure 5.** From top to bottom: AMS m/z 44 mass fraction, FTIR atomic O/C, FTIR organic hydroxyl fraction of OM (by mass), FTIR carboxylic acid fraction of OM (by mass), sum of XRF elements K, Ni, Ca, Fe, Sn, V, and Br (ng $m^{-3}$), AMS $SO_4^{2-}$ ($\mu$g $m^{-3}$), and FTIR OM ($\mu$g $m^{-3}$). For AMS $SO_4^{2-}$, the open squares have been omitted from the reported linear regression (solid line) to illustrate the southerly bias of AMS $O_4^{2-}$. The dashed line includes all AMS $SO_4^{2-}$.

AMS. These single particles were collected over a large geographical area and include measurements both near to and far from the continent making the small number of particles analyzed fairly representative of the regional submicron organic particle population.

[24] Sulfate composed a large fraction of the observed submicron mass and has anthropogenic and marine sources. Ion chromatography of 12–24 h filters was used to determine the average concentration of MSA (50 ± 22 ng $m^{-3}$). The continental sources of sulfate in South America include copper smelting, diesel, and coal combustion and appear to dominate the marine source of sulfate (oxidation of DMS) given the high coastal concentration of sulfate and the strong correlation with radon. In Figure 6b, the sum of inorganic sulfate (IC sulfate) and organic sulfate as in organosulfate groups ($COSO_3$) is compared with AMS sulfate. IC sulfate, unlike AMS sulfate, does not include organosulfate groups because IC sulfate is not fragmented before analysis. Sulfate from organosulfate groups is not distinguished from inorganic sulfate in the AMS due to fragmentation of the organosulfate molecule into an organic fragment and a sulfate fragment. A slightly more accurate CE for AMS sulfate is therefore determined by comparing it with the sum of organic and inorganic sulfate. The strong correlation (r = 0.98) and slope of 0.93 are consistent with the AMS CE of 1 for sulfate.

[25] Further evidence of organic and sulfate components occurring on different particle populations is given in Figure 8. The negative correlation (r = −0.85 for all air masses) of the organic acid fraction of $PM_1$ with the sulfate fraction of $PM_1$ indicates that the two components result from different sources. For CAM only, the inverse relationship is stronger (r = −0.92). Conversely, the acid fraction of $PM_1$ is mildly correlated to the dust fraction of $PM_1$ (r = 0.70) in all air masses and is more strongly correlated (r = 0.85) for CAM only. As expected, continental air masses show higher correlations among continental emissions than the XAM and MAM air masses in which other source types reduce the correlation. These relationships, combined with single particle measurements and the observed differences in AMS CE for organic and sulfate components, suggest that much of the organic mass was not present on sulfate-containing particles.

### 4.5. Combustion and Marine Organic Aerosol Factors

[26] Positive matrix factorization (PMF) was used to identify source factors from FTIR sample spectra [*Paatero and Tapper*, 1994] including only portions of the sample spectra with quantified peaks. One advantage of PMF is that the uncertainty associated with each measurement is included and used to constrain the determination of source factors. For each wave number, the standard deviation of the absorbance from all back filters was set as the measurement uncertainty. Results for 2, 3, 4, 5, and 6 factor solutions were explored and although the Q value (a normalized chi-square metric) was lowest for the six-factor solution, a two-factor solution was found to best represent the data. More than two factors resulted in factors that were not linearly independent. Also, the XRF elemental correlations with the additional factors in the three-, four-, five-, and six-factor solutions were nearly identical to the correlations with one of the two factors in the two-factor solution, indicating factor-splitting beyond two factors [*Ulbrich et al.*, 2009]. The two-factor solution was able to reproduce greater than 90% of the absorbance signal and greater than 75% of the organic mass, demonstrating that two factors are sufficient to represent most of the organic mixture features in the VOCALS-REx spectra. FPEAK (rotation) values from −0.4 to 0.4 were tested with the two-factor solution but no significant difference was found among the rotations; FPEAK = 0 is presented here as a representative example. The two source spectra are shown in Figure 9 along with their average composition determined by integrating the factor spectra following the method for ambient spectra. The "combustion" factor comprises mainly alkane (65%) and carboxylic acid (27%) groups and correlates with XRF measurements of sulfur, potassium, calcium, and metals while the "marine" factor is over 70% organic hydroxyl and either weakly or inversely (if at all) correlated to the same elements (Table 2). Vanadium was weakly correlated to marine OM and is emitted by residual oil combustion on ships and on land, so the small correlation observed is consistent with the inter-

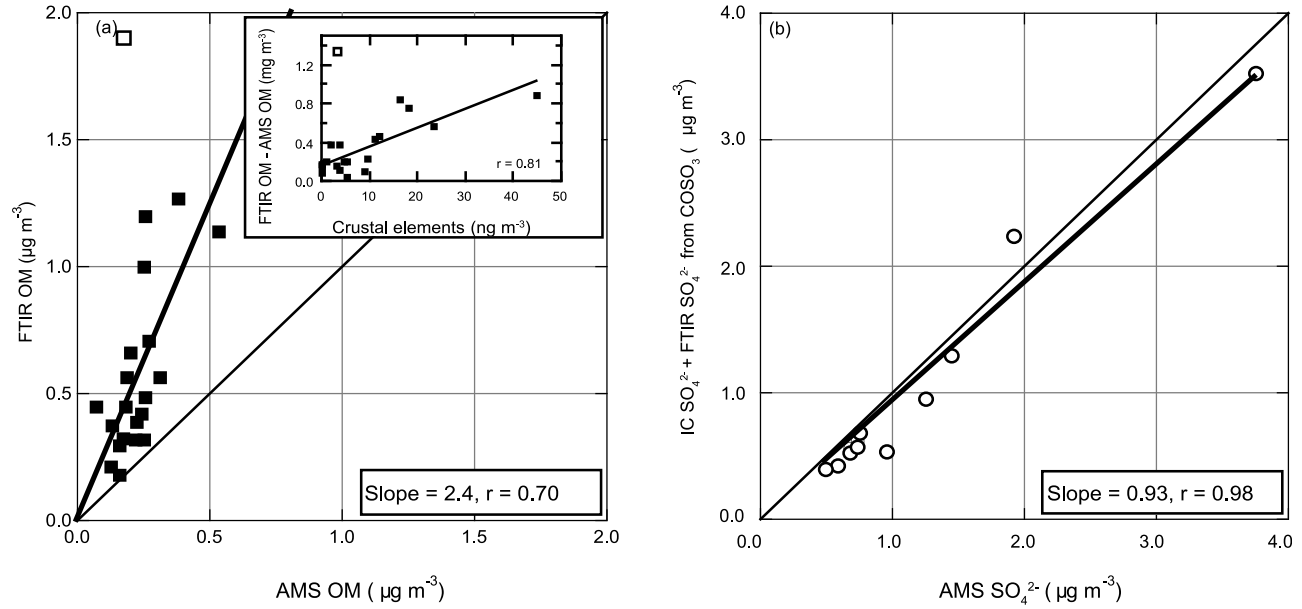


**Figure 6.** (a) Organic mass quantified from FTIR spectroscopy on Teflon filters is 2.4 times that measured by the Aerodyne AMS. AMS OM is averaged from the 5 min resolution data and includes only those points when the filters were sampling. Inset shows the difference in organic mass measured by FTIR spectroscopy (not including organosulfate), and AMS is correlated to the concentration of crustal components (nss-K, nss-Ca, Al, Si, Fe, and Ti). The open square in both graphs is not included in either linear regression to preserve the meaning of the calculated coefficients. (b) Comparison of the sum of IC nss-$SO_4^{2-}$ and FTIR organic sulfate from $COSO_3$ with AMS sulfate.

pretation of factor composition as "marine." Figure 4c shows the fraction of organic mass associated with each factor for October and November 2008. The combustion factor dominates the organic mass for most of the campaign. However, during some MAM periods, the fraction OM associated with the marine factor is greater than 50%, illustrating the importance of marine organic sources to total OM in the remote marine atmosphere.

## 5. Discussion

### 5.1. Continental Sources of Organic, Inorganic, and Elemental Components

[27] OM was an order of magnitude higher near the South American continent than in the remote marine atmosphere and correlations of OM with radon, sulfate and elements from dust or soil (Ca, Fe, and K), and industrial activities (S, V, Br, Ni, Sn) support an anthropogenic continental source of OM. Because air masses moved generally northward to the ship's location, measurements during CAM periods were likely influenced by urban centers along the Chilean coast south of the ship's track, such as Santiago. *Artaxo et al.* [1999] determined concentrations of elements in Santiago fine mode aerosol ($D_p < 2$ $\mu$m) using Particle-Induced X-ray Emission (PIXE). Samples were collected in two sites in downtown Santiago and several sources of $PM_2$ were identified by Absolute Principle Factor Analysis (APFA). The identified sources include sulfate (oxidized $SO_2$ from coal combustion) (64%), resuspended soil dust (15%), traffic emissions (16%), and oil combustion (2%). For consistency we will limit our comparison to elements in Table 1. Elements associated with the "Sulfates" factor are S, Sn, and K. Sn is not commonly found in urban aerosols but is particular to the soil in Chile which is enriched in Sn [*Artaxo et al.*, 1999]. Elements associated with "oil combustion" include Ni, V, and to a smaller extent, K, all of which were observed in our samples. Automobile and bus emissions are classified as the "Transport" factor and include Br, Sn, and K. Black carbon is most associated with the traffic emissions which are also the most likely anthropogenic source of organic compounds. Elements associated with the "Resuspended Soil Dust" factor are Ca and Fe. Resuspended soil dust in Santiago is contaminated with heavy metals and was observed by *Artaxo et al.* [1999] to be heavily mixed with traffic emissions. This observation is consistent with our single particle measurements of organic, carbonate, and potassium mixtures (Figure 7) and with the hypothesis that much of the organic mass was present on refractory particles (Figure 8b) rather than sulfate-containing particles. A second, biogenic continental source of OM from BVOC oxidation may exist in addition to anthropogenic sources described by *Artaxo et al.* [1999]. For example, *Elshorbany et al.* [2009] found that isoprene contributed 16% of the photochemically produced formaldehyde in Santiago, Chile. In this study, VOC measurements were not available to determine if isoprene or other biogenic VOCs contributed to continentally derived OM.

[28] Other cities along the Chilean and Peruvian coast are likely to contribute to the observed OM, sulfate, and elemental components but Santiago is a large and likely representative source of the regional anthropogenic aerosol particles with over 50 $\mu$g $m^{-3}$ $PM_2$ measured during the 1996 campaign. *Artaxo et al.* [1999] report sources of $PM_2$ specific to Santiago, Chile, that are similar to the measure-

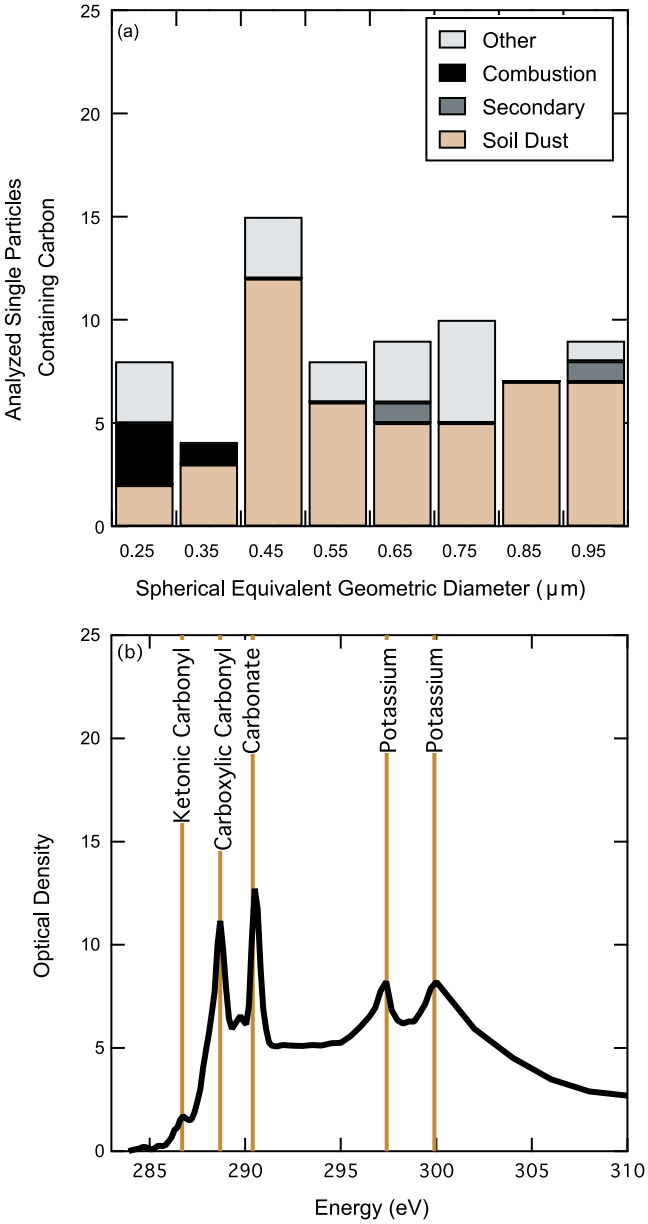


**Figure 7.** (a) The 96 organic-containing single particles identified by STXM-NEXAFS binned by 0.1 $\mu$m size increments. Bar height shows the total number of particles identified at each size. (b) Average spectrum of individual submicron organic-containing particles classified as "dust," normalized by the average optical density between 305 and 320 eV. The average absorption of the pre-K-edge portion of the spectrum (278–285 eV) was subtracted from all spectra. Vertical lines mark absorption peaks for organic and inorganic groups.

ments of inorganic and elemental components observed during VOCALS-REx. The proximity of Santiago to the back trajectories in the Continental samples and the magnitude of it as an emission source indicate that much of the observed organic mass associated with dust and metal components in our measurements originated from cities such as Santiago.

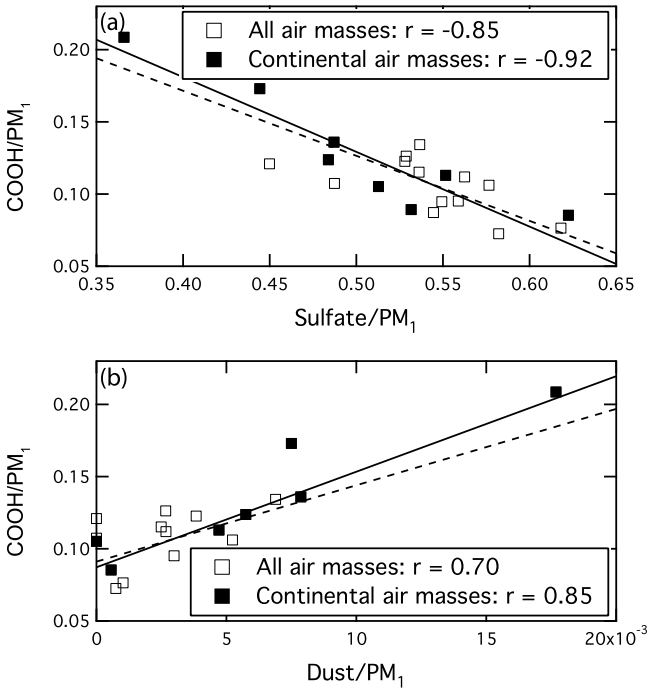


**Figure 8.** Comparison of acid fraction of $PM_1$ with (a) AMS sulfate and (b) dust fractions of $PM_1$.

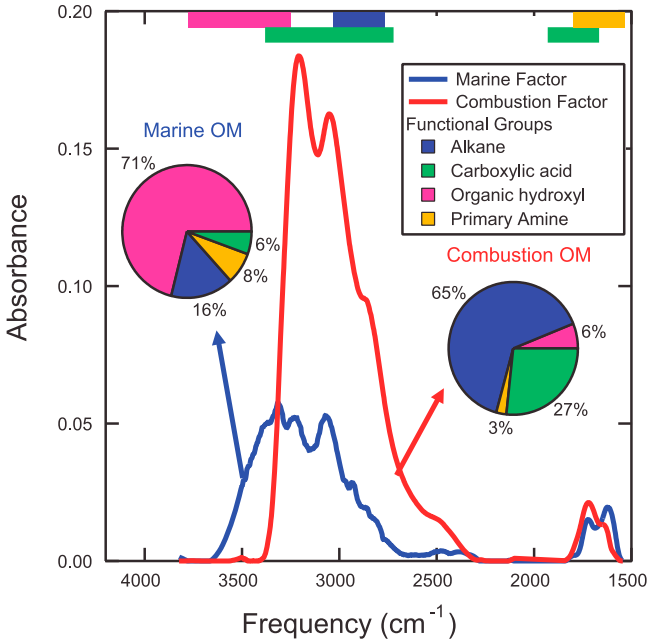


**Figure 9.** Positive matrix factorization of sample spectra resulted in two sources (marine and combustion) with representative FTIR spectra. As in Figure 3, colored bars across the top axis show the approximate range of absorbance of the functional groups. The average composition of each source is given in the two pie charts and corresponds to the values in Table 2.

**Table 2.** Organic Functional Group Composition and Elemental Correlations for Positive Matrix Factorization Two-Factor Analysis[a]

| | Marine Factor | Combustion Factor |
|---|---|---|
| Average OM | 0.11 ± 0.07 | 0.4 ± 0.3 |
| Organic composition (% mass) | | |
| Alkane | 16% | 65% |
| Carboxylic acid | 6% | 27% |
| Organic hydroxyl | 71% | 6% |
| Amine | 8% | 3% |
| Elemental correlations (r) | | |
| S | −0.22 | 0.94 |
| V | 0.24 | 0.74 |
| Sn | – | 0.69 |
| K | – | 0.6 |
| Br | – | 0.82 |
| Ni | – | 0.28 |
| Ca | – | 0.38 |
| Fe | – | 0.62 |

[a]Correlations stronger than 0.2 (and −0.2) are shown.

### 5.2. Marine Sources of Organic Components

[29] During MAM periods and some XAM periods, OM was as low as 0.2 $\mu$g m$^{-3}$ and had a significantly different functional group composition from CAM periods. The organic mass observed during MAM periods was dominated by the "marine" factor, but was not purely biogenic marine OM given the small but detectable amounts of ship emission tracers (Fe and V) in the submicron particles. Organic hydroxyl groups composed 71% of OM associated with the marine factor compared to only 6% of OM in the combustion factor and are found in polysaccharides and fatty alcohol molecules which, in addition to fatty acids, are some of the molecule types thought to be concentrated on the ocean's surface [*Aluwihare et al.*, 1997]. Biogenic organic compounds on the ocean's surface can be emitted to the atmosphere during bubble bursting [*Blanchard and Syzdek*, 1970; *Hoffman and Duce*, 1977; *Tseng et al.*, 1992; *Mochida et al.*, 2002; *O'Dowd et al.*, 2004; *Cavalli et al.*, 2004; *Leck and Bigg*, 2005; *Russell et al.*, 2010]. *Russell et al.* [2010] show a large contribution from a similar PMF-derived marine OM in the Arctic and North Atlantic and positive correlations between marine OM and sea salt. In addition, comparisons of PMF-derived marine factors (including the marine factor presented here) to reference disaccharides and polysaccharides imply very similar composition, with large contributions from organic hydroxyl to the total organic mass [*Russell et al.*, 2010].

### 5.3. Effect of Mixing Combustion and Marine Oxygenated Organic Aerosol on O/C

[30] Observations of organic aerosols close to and more distant from particle sources generally show an increase in oxygenated groups such as carboxylic acids and a decrease in hydrophobic groups such as alkenes and alkanes with distance from source [*Maria et al.*, 2004; *Zhang et al.*, 2007; *Gilardoni et al.*, 2007]. Quantifying transformations of organic aerosol components such as oxidation of alkane, alkene, and aromatic groups to organic hydroxyl and carboxylic acid groups is often complicated in remote regions when multiple sources are mixed during transport and because some transformations are more rapid than others [*Volkamer et al.*, 2006]. A simplified proxy for photochemical aging is the atomic O/C ratio of organic aerosols, which increases with photochemical age due to an increasing fraction of oxidized chemical groups [*Zhang et al.*, 2007; *DeCarlo et al.*, 2007, 2008; *Russell et al.*, 2009a]. The usefulness of O/C in organic aerosol measurements has resulted in new efforts to measure O/C at high time resolution with the Aerodyne Aerosol Mass Spectrometer [*Aiken et al.*, 2007, 2008; *DeCarlo et al.*, 2007]. Elemental analysis (EA) of high-resolution (HR) mass spectra shows fairly good agreement with atomic O/C and H/C ratios for laboratory standards, although O/C in groups such as organic hydroxyl were underpredicted by as much as 50% [*Aiken et al.*, 2007]. The observed O/C ratio during VOCALS-REx from organic functional groups (FTIR) agrees with O/C estimated from the mass fraction of m/z 44 (AMS) for samples with the lowest organic hydroxyl group fractions (<15%), but is up to 5 times larger in samples with greater than 30% organic hydroxyl groups. This difference is most important in the more remote samples which have a smaller contribution from continental OM and larger contribution from marine OM, and therefore a larger fraction of organic hydroxyl groups. A recent comparison of organic functional groups and organic mass fragments has shown weak correlations between both carboxylic acid and organic hydroxyl groups and m/z 44 fraction [*Russell et al.*, 2009b]. Further, because O/C of the organic aerosol does not change significantly in the remote atmosphere it is not a relevant metric for photochemical age of transported particles. Consequently O/C does not represent a relevant metric for changes in the composition from atmospheric processing and is unlikely to provide a direct proxy for CCN activity or other aerosol properties.

### 5.4. Aqueous-Phase Formation of Organosulfate Groups

[31] The contribution of SOA to total organic aerosol mass is variable even on small time and spatial scales and depends on a large number of factors including gas phase precursor concentrations, oxidant levels, time of day, and preexisting aerosol [*Odum et al.*, 1996; *Maria et al.*, 2004; *Donahue et al.*, 2005], making model predictions of SOA challenging and often inaccurate when compared with measurements [*Heald et al.*, 2005; *De Gouw et al.*, 2005; *Volkamer et al.*, 2006; *Robinson et al.*, 2007]. Identifying, separating, and quantifying SOA in ambient mixtures of primary and secondary organic aerosol is therefore a key step toward understanding the major formation pathways and the top parameters controlling SOA production. Recently several studies have highlighted the potentially important role of organosulfate formation in increasing SOA yield by increasing partitioning of semivolatile organic compounds (SVOCs) into the particle phase [*Romero and Oehme*, 2005; *Iinuma et al.*, 2007a, 2007b; *Surratt et al.*, 2007a, 2007b, 2008; *Lukács et al.*, 2009; *Altieri et al.*, 2009; *Minerath and Elrod*, 2009; *Iinuma et al.*, 2009; *Claeys et al.*, 2009]. *Claeys et al.* [2009] found organosulfate compounds in fine aerosol in a marine environment with little continental influence, illustrating the importance of primary marine organic sources (fatty acid residues) and DMS-derived sulfate when no pollution sources exist. *Galloway et al.* [2009] identified organosulfate compounds

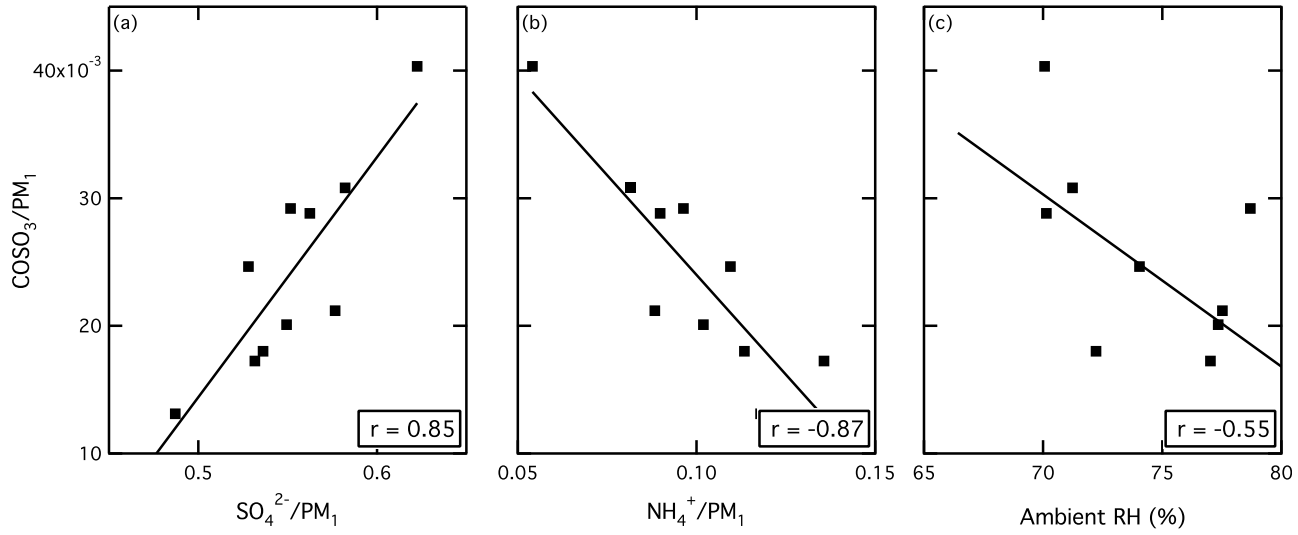


**Figure 10.** Comparison of organosulfate fraction of $PM_1$ with (a) AMS sulfate and (b) AMS ammonium fractions of $PM_1$. (c) Comparison of organosulfate fraction of $PM_1$ with ambient RH (%).

in laboratory aerosol particles from reactive uptake of glyoxal onto ammonium sulfate seed aerosol under irradiated conditions. *Altieri et al.* [2009] found organosulfate compounds in rainwater samples that contained other compounds characteristic of SOA, such as organic acids. However, few quantitative ambient measurements of organosulfate compounds or groups exist, providing little basis for estimating the atmospheric importance of organosulfate groups relative to other secondary organic aerosol products, such as carboxylic acids [*Maria and Russell*, 2005; *Gilardoni et al.*, 2007; *Surratt et al.*, 2008; *Lukács et al.*, 2009; *Russell et al.*, 2009a]. Size-segregated measurements of organosulfate in rural fine aerosol particles collected in Hungary show a peak in estimated organosulfate concentration (6–14% of total sulfate) for particle diameters near 400 nm coinciding with the typical peak in effective surface size distribution [*Lukács et al.*, 2009], consistent with proposed heterogeneous mechanisms from laboratory studies [*Surratt et al.*, 2007a, 2007b; *Minerath and Elrod*, 2009; *Iinuma et al.*, 2009]. For the same study, *Surratt et al.* [2008] estimate that the organosulfate contribution to the total organic mass could be as high as 30%.

[32] VOCALS-REx organosulfate group concentrations were more strongly associated with continental emissions than marine organics with 51 ng $m^{-3}$ in CAM, 29 ng $m^{-3}$ in XAM and 15 ng $m^{-3}$ in MAM and composed up to 13% of OM and up to 9% of total sulfate. Our measurements show a strong positive correlation (r = 0.85) between organosulfate and sulfate fractions of $PM_1$ (Figure 10a) and a strong inverse correlation (r = −0.87) between organosulfate and ammonium fractions of $PM_1$ (Figure 10b), consistent with both particle-phase formation by reaction with condensed sulfate and acid catalysis. The highest observed organosulfate concentration coincided with the peak sulfate concentration and the highest ratio of sulfate to ammonium measured. This is consistent with observations from *Surratt et al.* [2007a] and *Minerath and Elrod* [2009] of increased SOA yield with increasing acidity due to an acid hydrolysis mechanism for organosulfate formation of biogenic VOC oxidation products (epoxides). VOC precursors for organosulfate are most likely continental given the higher concentration of OM and specifically organosulfate groups in CAM. However, speciated VOC measurements are not available for the study period so it is not possible to separate biogenic and anthropogenic continental sources. Biogenic VOCs have been identified in Santiago, Chile [*Elshorbany et al.*, 2009] though their contribution to formaldehyde was estimated to be only 16%.

[33] Laboratory studies with glyoxal and inorganic seed aerosol under dark conditions by *Liggio et al.* [2005] show a stronger relationship between relative humidity (RH) and SOA yield than particle acidity. They observed little SOA formation below 50% RH, which they attribute to a reaction mechanism requiring aqueous dissolution of the organic VOC (i.e., glyoxal) prior to reaction. A significant increase in SOA yield was observed above 50% RH, however, at very high RH (above 80%) a small decrease in SOA yield was observed. This trend was attributed to the dilution of the hydrated glyoxal available as reactant and the reduction of the particle acidity. Figure 10c shows the inverse relationship between organosulfate fraction of $PM_1$ with ambient relative humidity (r = −0.55) above 65% RH consistent with *Liggio et al.* [2005].

[34] HYSPLIT back trajectories shown in Figure 2 indicate that even CAM samples had spent two to three days in the stratocumulus-topped MBL so cloud processing may also play a role in the observed organosulfate group concentrations. Other work has shown that cloud and fog processing may play a significant role in SOA formation through aqueous phase photooxidation of organic components [*Blando and Turpin*, 2000; *Sorooshian et al.*, 2007; *Perri et al.*, 2009]. The VOCALS results are consistent with the role of aqueous particles in organosulfate production, but they suggest that higher amounts of liquid water associated with some cloud conditions may reduce the yield of organosulfate. However, ambient relative humidity was correlated with the ratio of ammonium to sulfate (r = 0.71) such that the driest conditions coincidentally had the most

acidic sulfate aerosol. The tighter correlations of organosulfate fraction with sulfate implies that particle acidity had a more direct relationship with organosulfate formation than ambient RH for VOCALS-REx conditions (which were all at RH > 50%). The observed trends in VOCALS-REx organosulfate concentration suggest that in regions with similar conditions (i.e., RH above 50%, high sulfate concentrations relative to ammonium, and elevated VOC concentrations) organosulfate may have a significant contribution to SOA mass.

## 6. Conclusion

[35] Organic functional groups measured in submicron particles showed higher carboxylic acid fractions (and lower organic hydroxyl fractions) in CAM than in MAM and no measurable change in O/C ratio with radon or distance from the continent, consistent with oxygenated organic groups from both marine and continental sources. OM associated with continental tracers such as radon, sulfate, and dust elements was on average 4 times that observed during periods of very low continental influence. In the most remote sampling location, OM associated with the marine factor was greater than 50% of the total OM measured by FTIR spectroscopy. Satellite measurements support the hypothesis that continental outflow is a significant source of aerosol to the region around 20°S; in situ measurements give estimated particle concentrations for the satellite AOD, while providing detailed size and chemistry information. A comparison of OM and O/C from FTIR spectroscopy and AMS showed that the AMS may have a reduced CE for organic mass on refractory particles and that m/z 44 fraction of OM may not accurately predict atomic O/C when organic hydroxyl composes a large fraction of OM.

[36] Measurements in CAM show a strong positive correlation between carboxylic acid fraction and dust fractions of $PM_1$ and a strong negative correlation between carboxylic acid and sulfate fractions of $PM_1$, consistent with observed differences in AMS CE for organic and sulfate that indicate external mixtures of the two components. Previous measurements of submicron aerosol within Santiago show similar elemental signatures to those measured on board NOAA R/V *Ronald H. Brown* supporting the identification of this large source of $PM_1$. Organosulfate groups were frequently present in significant fractions of OM (3–13%) and correlated positively with sulfate fraction and inversely with ammonium fraction and ambient relative humidity, consistent with previously reported ambient and laboratory studies. Additional measurements of organic functional group concentrations would provide a more detailed, quantitative understanding of the sources and processes controlling submicron organic mass in the southeast Pacific MBL.

[37] **Acknowledgments.** This work was supported by NSF grant ATM-0744636. P.K.Q., T.S.B., and D.S.C. were supported by the NOAA Climate Project Office, Atmospheric Composition and Climate Program. The authors would like to acknowledge Shang Liu for analysis of single particles by STXM-NEXAFS and Satoshi Takahama for technical assistance with STXM and PMF analyses. We would also like to thank Derek Coffman, James Johnson, and Catherine Hoyle for their assistance in sample collection and analysis as well as the captain and crew of the NOAA R/V *Ronald H. Brown* for their support in the field.

## References

Aiken, A. C., P. F. DeCarlo, and J. L. Jimenez (2007), Elemental analysis of organic species with electron ionization high-resolution mass spectrometry, *Anal. Chem.*, *79*(21), 8350–8358, doi:10.1021/ac071150w.

Aiken, A. C., et al. (2008), O/C and OM/OC ratios of primary, secondary, and ambient organic aerosols with high-resolution time-of-flight aerosol mass spectrometry, *Environ. Sci. Technol.*, *42*(12), 4478–4485, doi:10.1021/es703009q.

Alfarra, M. R., et al. (2004), Characterization of urban and rural organic particulate in the lower Fraser Valley using two aerodyne aerosol mass spectrometers, *Atmos. Environ.*, *38*(34), 5745–5758, doi:10.1016/j.atmosenv.2004.01.054.

Allan, J. D., et al. (2004), Submicron aerosol composition at Trinidad Head, California, during ITCT 2K2: Its relationship with gas phase volatile organic carbon and assessment of instrument performance, *J. Geophys. Res.*, *109*, D23S24, doi:10.1029/2003JD004208.

Altieri, K. E., B. J. Turpin, and S. P. Seitzinger (2009), Oligomers, organosulfates, and nitrooxy organosulfates in rainwater identified by ultra-high resolution electrospray ionization FT-ICR mass spectrometry, *Atmos. Chem. Phys.*, *9*, 2533–2542, doi:10.5194/acp-9-2533-2009.

Aluwihare, L. I., D. J. Repeta, and R. F. Chen (1997), A major biopolymeric component to dissolved organic carbon in surface sea water, *Nature*, *387*(6629), 166–169.

Andreae, M. O. (2009), Correlation between cloud condensation nuclei concentration and aerosol optical thickness in remote and polluted regions, *Atmos. Chem. Phys.*, *9*, 543–556.

Artaxo, P., P. Oyola, and R. Martinez (1999), Aerosol composition and source apportionment in Santiago de Chile, *Nucl. Instrum. Methods Phys. Res., Sect. B*, *150*(1), 409–416.

Bates, T. S., P. K. Quinn, D. S. Covert, D. J. Coffman, J. E. Johnson, and A. Wiedensohler (2000), Aerosol physical properties and processes in the lower marine boundary layer: a comparison of shipboard sub-micron data from ACE-1 and ACE-2, *Tellus, Ser. B*, *52*(2), 258–272.

Bates, T. S., P. K. Quinn, D. J. Coffman, J. E. Johnson, and A. M. Middlebrook (2005), Dominance of organic aerosols in the marine boundary layer over the Gulf of Maine during NEAQS 2002 and their role in aerosol light scattering, *J. Geophys. Res.*, *110*, D18202, doi:10.1029/2005JD005797.

Bates, T. S., et al. (2008), Boundary layer aerosol chemistry during TexAQS/GoMACCS 2006: Insights into aerosol sources and transformation processes, *J. Geophys. Res.*, *113*, D00F01, doi:10.1029/2008JD010023.

Blanchard, D. C., and L. Syzdek (1970), Mechanism for the water-to-air transfer and concentration of bacteria, *Science*, *170*(3958), 626–628.

Blando, J. D., and B. J. Turpin (2000), Secondary organic aerosol formation in cloud and fog droplets: A literature evaluation of plausibility, *Atmos. Environ.*, *34*(10), 1623–1632.

Bretherton, C. S., T. Uttal, C. W. Fairall, S. E. Yuter, R. A. Weller, D. Baumgardner, K. Comstock, R. Wood, and G. B. Raga (2004), The EPIC 2001 stratocumulus study, *Bull. Am. Meteorol. Soc.*, *85*(7), 967–977.

Cavalli, F., et al. (2004), Advances in characterization of size-resolved organic matter in marine aerosol over the North Atlantic, *J. Geophys. Res.*, *109*, D24215, doi:10.1029/2004JD005137.

Claeys, M., et al. (2009), Chemical characterisation of marine aerosol at Amsterdam Island during the austral summer of 2006–2007, *J. Aerosol Sci.*, doi:10.1016/j.jaerosci.2009.08.003.

DeCarlo, P. F., et al. (2007), Fast airborne aerosol size and chemistry measurements with the high resolution aerosol mass spectrometer during the MILAGRO Campaign, *Atmos. Chem. Phys. Discuss*, *7*, 18,269–18,317, doi:10.5194/acpd-7-18269-2007.

DeCarlo, P. F., et al. (2008), Fast airborne aerosol size and chemistry measurements above Mexico City and Central Mexico during the MILAGRO campaign, *Atmos. Chem. Phys.*, *8*, 4027–4048, doi:10.5194/acp-8-4027-2008.

De Gouw, J. A., et al. (2005), Budget of organic carbon in a polluted atmosphere: Results from the New England Air Quality Study in 2002, *J. Geophys. Res.*, *110*, D16305, doi:10.1029/2004JD005623.

Donahue, N. M., K. E. H. Hartz, B. Chuong, A. A. Presto, C. O. Stanier, T. Rosenhørn, A. L. Robinson, and S. N. Pandis (2005), Critical factors determining the variation in SOA yields from terpene ozonolysis: A combined experimental and computational study, *Faraday Discuss.*, *130*, 295–309, doi:10.1039/b417369d.

Drewnick, F., J. J. Schwab, O. Hogrefe, S. Peters, L. Husain, D. Diamond, R. Weber, and K. L. Demerjian (2003), Intercomparison and evaluation of four semi-continuous PM2.5 sulfate instruments, *Atmos. Environ.*, *37*(24), 3335–3350, doi:10.1016/S1352-2310(03)00351.

Elshorbany, Y. F., et al. (2009), Oxidation capacity of the city air of Santiago, Chile, *Atmos. Chem. Phys*, *9*, 2257–2273.

Ervens, B., G. Feingold, and S. M. Kreidenweis (2005), Influence of water-soluble organic carbon on cloud drop number concentration, *J. Geophys. Res.*, *110*, D18211, doi:10.1029/2004JD005634.

Galloway, M. M., P. S. Chhabra, A. W. H. Chan, J. D. Surratt, R. C. Flagan, J. H. Seinfeld, and F. N. Keutsch (2009), Glyoxal uptake on ammonium sulphate seed aerosol: reaction products and reversibility of uptake under dark and irradiated conditions, *Atmos. Chem. Phys*, *9*, 3331–3345.

Garreaud, R. D., and R. C. Muñoz (2005), The low-level jet off the west coast of subtropical South America: Structure and variability, *Mon. Weather Rev.*, *133*(8), 2246–2261, doi:10.1175/MWR2972.1.

Gilardoni, S., et al. (2007), Regional variation of organic functional groups in aerosol particles on four US east coast platforms during the International Consortium for Atmospheric Research on Transport and Transformation 2004 campaign, *J. Geophys. Res.*, *112*, D10S27, doi:10.1029/2006JD007737.

Gilardoni, S., et al. (2009), Characterization of organic ambient aerosol during MIRAGE 2006 on three platforms, *Atmos. Chem. Phys.*, *9*, 5417–5432, doi:10.5194/acpd-9-6617-2009.

Hawkins, L. N., L. M. Russell, C. H. Twohy, and J. R. Anderson (2008), Uniform particle-droplet partitioning of 18 organic and elemental components measured in and below DYCOMS-II stratocumulus clouds, *J. Geophys. Res.*, *113*, D14201, doi:10.1029/2007JD009150.

Heald, C. L., D. J. Jacob, R. J. Park, L. M. Russell, B. J. Huebert, J. H. Seinfeld, H. Liao, and R. J. Weber (2005), A large organic aerosol source in the free troposphere missing from current models, *Geophys. Res. Lett.*, *32*, L18809, doi:10.1029/2005GL023831.

Hoffman, E. J., and R. A. Duce (1977), Organic carbon in marine atmospheric particulate matter: Concentration and particle size distribution, *Geophys. Res. Lett.*, *4*(10), 449–452.

Huneeus, N., L. Gallardo, and J. A. Rutllant (2006), Offshore transport episodes of anthropogenic sulfur in northern Chile: Potential impact on the stratocumulus cloud deck, *Geophys. Res. Lett.*, *33*, L19819, doi:10.1029/2006GL026921.

Iinuma, Y., C. Müller, O. Böge, T. Gnauk, and H. Herrmann (2007a), The formation of organic sulfate esters in the limonene ozonolysis secondary organic aerosol (SOA) under acidic conditions, *Atmos. Environ.*, *41*(27), 5571–5583.

IInuma, Y., C. Müller, T. Berndt, O. Böge, M. Claeys, and H. Herrmann (2007b), Evidence for the existence of organosulfates from beta 2-pinene nzonolysis in ambient secondary organic aerosol, *Environ. Sci. Technol.*, *41*(19), 6678–6683.

Iinuma, Y., O. Böge, A. Kahnt, and H. Herrmann (2009), Laboratory chamber studies on the formation of organosulfates from reactive uptake of monoterpene oxides, *Phys. Chem. Chem. Phys.*, *11*(36), 7985–7997.

Jayne, J. T., D. C. Leard, X. Zhang, P. Davidovits, K. A. Smith, C. E. Kolb, and D. R. Worsnop (2000), Development of an aerosol mass spectrometer for size and composition analysis of submicron particles, *Aerosol Sci. Technol.*, *33*(1), 49–70.

Jimenez, J. L., et al. (2003), Ambient aerosol sampling using the aerodyne aerosol mass spectrometer, *J. Geophys. Res.*, *108*(D7), 8425, doi:10.1029/2001JD001213.

Johnson, K. S., B. Zuberi, L. T. Molina, M. J. Molina, M. J. Iedema, J. P. Cowin, D. J. Gaspar, C. Wang, and A. Laskin (2005), Processing of soot in an urban environment: Case study from the Mexico City metropolitan area, *Atmos. Chem. Phys.*, *5*, 3033–3043, doi:1680-7324/acp/2005-5-3033.

Leck, C., and E. K. Bigg (2005), Source and evolution of the marine aerosol–A new perspective, *Geophys. Res. Lett.*, *32*, L19803, doi:10.1029/2005GL023651.

Liggio, J., S. M. Li, and R. McLAREN (2005), Heterogeneous reactions of glyoxal on particulate matter: Identification of acetals and sulfate esters, *Environ. Sci. Technol.*, *39*(6), 1532–1541, doi:10.1021/es048375y.

Liu, S., S. Takahama, L. M. Russell, S. Gilardoni, and D. Baumgardner (2009), Oxygenated organic functional groups and their sources in single and submicron organic particles in MILAGRO 2006 campaign, *Atmos. Chem. Phys. Discuss.*, *9*, 4567–4607, doi:10.5194/acp-9-6849-2009.

Lukács, H., A. Gelencsér, A. Hoffer, G. Kiss, K. Horváth, and Z. Hartyáni (2009), Quantitative assessment of organosulfates in size-segregated rural fine aerosol, *Atmos. Chem. Phys.*, *9*, 231–238, doi:10.5194/acp-9-231-2009.

Maria, S. F., and L. M. Russell (2005), Organic and inorganic aerosol below-cloud scavenging by suburban New Jersey precipitation, *Environ. Sci. Technol.*, *39*(13), 4793–4800, doi:10.1021/es0491679.

Maria, S. F., L. M. Russell, B. J. Turpin, and R. J. Porcja (2002), FTIR measurements of functional groups and organic mass in aerosol samples over the Caribbean, *Atmos. Environ.*, *36*(33), 5185–5196.

Maria, S. F., L. M. Russell, B. J. Turpin, R. J. Porcja, T. L. Campos, R. J. Weber, and B. J. Huebert (2003), Source signatures of carbon monoxide and organic functional groups in Asian Pacific Regional Aerosol Characterization Experiment (ACE-Asia) submicron aerosol types, *J. Geophys. Res.*, *108*(D23), 8637, doi:10.1029/2003JD003703.

Maria, S. F., L. M. Russell, M. K. Gilles, and S. C. B. Myneni (2004), Organic aerosol growth mechanisms and their climate-forcing implications, *Science*, *306*(5703), 1921–1924, doi:10.1126/science.1103491.

Matthew, B. M., A. M. Middlebrook, and T. B. Onasch (2008), Collection efficiencies in an Aerodyne aerosol mass spectrometer as a function of particle phase for laboratory generated aerosols, *Aerosol Sci. Technol.*, *42*(11), 884–898, doi:10.1080/02786820802356797.

Minerath, E. C., and M. J. Elrod (2009), Assessing the potential for diol and hydroxy sulfate ester formation from the reaction of epoxides in tropospheric aerosols, *Environ. Sci. Technol.*, *43*(5), 1386–1392.

Mochida, M., Y. Kitamori, K. Kawamura, Y. Nojiri, and K. Suzuki (2002), Fatty acids in the marine atmosphere: Factors governing their concentrations and evaluation of organic films on sea-salt particles, *J. Geophys. Res.*, *107*(D17), 4325, doi:10.1029/2001JD001278.

O'Dowd, C. D., E. Becker, and M. Kulmala (2001), Mid-latitude North-Atlantic aerosol characteristics in clean and polluted air, *Atmos. Res.*, *58*(3), 167–185.

O'Dowd, C. D., M. C. Facchini, F. Cavalli, D. Ceburnis, M. Mircea, S. Decesari, S. Fuzzi, Y. J. Yoon, and J. P. Putaud (2004), Biogenically driven organic contribution to marine aerosol, *Nature*, *431*(7009), 676–680, doi:10.1038/nature02959.

Odum, J. R., et al. (1996), Gas/particle partitioning and secondary organic aerosol yields, *Environ. Sci. Technol.*, *30*(8), 2580–2585.

Paatero, P., and U. Tapper (1994), Positive matrix factorization: A non-negative factor model with optimal utilization of error estimates of data values, *Environmetrics*, *5*(2), 111–126.

Perri, M. J., S. Seitzinger, and B. J. Turpin (2009), Secondary organic aerosol production from aqueous photooxidation of glycolaldehyde: Laboratory experiments, *Atmos. Environ.*, *43*(8), 1487–1497, doi:10.1016/j.atmosenv.2008.11.037.

Pirjola, L., C. D. O'Dowd, I. M. Brooks, and M. Kulmala (2000), Can new particle formation occur in the clean marine boundary layer?, *J. Geophys. Res.*, *105*(D21), 26,531–26,546.

Prenni, A. J., M. D. Petters, S. M. Kreidenweis, P. J. DeMott, and P. J. Ziemann (2007), Cloud droplet activation of secondary organic aerosol, *J. Geophys. Res.*, *112*, D10223, doi:10.1029/2006JD007963.

Quinn, P. K., V. N. Kapustin, T. S. Bates, and D. S. Covert (1996), Chemical and optical properties of marine boundary layer aerosol particles of the mid-Pacific in relation to sources and meteorological transport, *J. Geophys. Res.*, *101*(D3), 6931–6951, doi:10.1029/95JD03444.

Quinn, P. K., et al. (2006), Impacts of sources and aging on submicrometer aerosol properties in the marine boundary layer across the Gulf of Maine, *J. Geophys. Res.*, *111*, D23S36, doi:10.1029/2006JD007582.

Quinn, P. K., T. S. Bates, D. J. Coffman, and D. S. Covert (2008), Influence of particle size and chemistry on the cloud nucleating properties of aerosols, *Atmos. Chem. Phys.*, *8*, 1029–1042, doi:10.5194/acpd-7-14171-200.

Remer, L. A., et al. (2002), Validation of MODIS aerosol retrieval over ocean, *Geophys. Res. Lett.*, *29*(12), 8008, doi:10.1029/2001GL013204.

Richter, I., and C. R. Mechoso (2006), Orographic influences on subtropical stratocumulus, *J. Atmos. Sci.*, *63*(10), 2585–2601, doi:10.1175/JAS3756.1.

Robinson, A. L., N. M. Donahue, M. K. Shrivastava, E. A. Weitkamp, A. M. Sage, A. P. Grieshop, T. E. Lane, J. R. Pierce, and S. N. Pandis (2007), Rethinking organic aerosols: Semivolatile emissions and photochemical aging, *Science*, *315*(5816), 1259–1262, doi:10.1126/science.1133061.

Romero, F., and M. Oehme (2005), Organosulfates–A new component of humic-like substances in atmospheric aerosols?, *J. Atmos. Chem.*, *52*(3), 283–294.

Russell, L. M. (2003), Aerosol organic-mass-to-organic-carbon ratio measurements, *Environ. Sci. Technol.*, *37*(13), 2982–2987.

Russell, L. M., S. Takahama, S. Liu, L. N. Hawkins, D. S. Covert, P. K. Quinn, and T. S. Bates (2009a), Oxygenated fraction and mass of organic aerosol from direct emission and atmospheric processing measured on the R/V *Ronald Brown* during TEXAQS/GoMACCS 2006, *J. Geophys. Res.*, *114*, D00F05, doi:10.1029/2008JD011275.

Russell, L. M., R. Bahadur, L. N. Hawkins, J. Allan, D. Baumgardner, P. K. Quinn, and T. S. Bates (2009b), Organic aerosol characterization by complementary measurements of chemical bonds and molecular fragments, *Atmos. Environ.*, *43*(38), 6100–6105.

Russell, L. M., L. N. Hawkins, A. M. Frossard, P. K. Quinn, and T. S. Bates (2010), Carbohydrate-like composition of submicron atmospheric particles and their production from ocean bubble bursting, *Proc. Natl. Acad. Sci. U. S. A.*, *107*, 6652–6657, doi:10.1073/pnas.0908905107.

Seinfeld, J. H., G. B. Erdakos, W. E. Asher, and J. F. Pankow (2001), Modeling the formation of secondary organic aerosol (SOA). 2. The

predicted effects of relative humidity on aerosol formation in the $\alpha$-pinene-, $\beta$-pinene-, sabinene-, $\delta$ 3-carene-, and cyclohexene-ozone systems, *Environ. Sci. Technol.*, *35*(9), 1806–1817, doi:10.1021/es001765.

Sorooshian, A., M. L. Lu, F. J. Brechtel, H. Jonsson, G. Feingold, R. C. Flagan, and J. H. Seinfeld (2007), On the source of organic acid aerosol layers above clouds, *Environ. Sci. Technol.*, *41*(13), 4647–4654, doi:10.1021/es0630442.

Surratt, J. D., M. Lewandowski, J. H. Offenberg, M. Jaoui, T. E. Kleindienst, E. O. Edney, and J. H. Seinfeld (2007a), Effect of acidity on secondary organic aerosol formation from isoprene, *Environ. Sci. Technol.*, *41*(15), 5363–5369, doi:10.1021/es0704176.

Surratt, J. D., et al. (2007b), Evidence for organosulfates in secondary organic aerosol, *Environ. Sci. Technol.*, *41*(2), 517–527, doi:10.1021/es062081q.

Surratt, J. D., et al. (2008), Organosulfate formation in biogenic secondary organic aerosol, *J. Phys. Chem. A*, *112*(36), 8345–8378.

Takahama, S., S. Gilardoni, L. M. Russell, and A. L. D. Kilcoyne (2007), Classification of multiple types of organic carbon composition in atmospheric particles by scanning transmission X-ray microscopy analysis, *Atmos. Environ.*, *41*(40), 9435–9451, doi:10.1016/j.atmosenv.2007.08.051.

Takahama, S., S. Liu, and L. M. Russell (2010), Coatings and clusters of carboxylic acids in carbon-containing atmospheric particles from spectromicroscopy and their implications for cloud-nucleating and optical properties, *J. Geophys. Res.*, *115*, D01202, doi:10.1029/2009JD012622.

Tseng, R., J. T. Viechnicki, R. A. Skop, and J. W. Brown (1992), Sea-to-air transfer of surface-active organic compounds by bursting bubbles, *J. Geophys. Res.*, *97*(C4), 5201–5206.

Twohy, C. H., M. D. Petters, J. R. Snider, B. Stevens, W. Tahnk, M. Wetzel, L. Russell, and F. Burnet (2005), Evaluation of the aerosol indirect effect in marine stratocumulus clouds: Droplet number, size, liquid water path, and radiative impact, *J. Geophys. Res.*, *110*, D08203, doi:10.1029/2004JD005116.

Ulbrich, I. M., M. R. Canagaratna, Q. Zhang, D. R. Worsnop, and J. L. Jimenez (2009), Interpretation of organic components from positive matrix factorization of aerosol mass spectrometric data, *Atmos. Chem. Phys.*, *9*, 2891–2918, doi:10.5194/acp-9-2891-2009.

Volkamer, R., J. L. Jimenez, F. San Martini, K. Dzepina, Q. Zhang, D. Salcedo, L. T. Molina, D. R. Worsnop, and M. J. Molina (2006), Secondary organic aerosol formation from anthropogenic air pollution: Rapid and higher than expected, *Geophys. Res. Lett.*, *33*, L17811, doi:10.1029/2006GL026899.

Ward, J. H., Jr. (1963), Hierarchical grouping to optimize an objective function, *J. Am. Stat. Assoc.*, *58*, 236–244.

Zhang, Q., D. R. Worsnop, M. R. Canagaratna, and J. L. Jimenez (2005a), Hydrocarbon-like and oxygenated organic aerosols in Pittsburgh: Insights into sources and processes of organic aerosols, *Atmos. Chem. Phys.*, *5*, 3289–3311, doi:10.5194/acp-5-3289-2005.

Zhang, Q., M. R. Canagaratna, J. T. Jayne, D. R. Worsnop, and J. L. Jimenez (2005b), Time-and size-resolved chemical composition of submicron particles in Pittsburgh: Implications for aerosol sources and processes, *J. Geophys. Res.*, *110*, D07S09, doi:10.1029/2004JD004649.

Zhang, Q., et al. (2007), Ubiquity and dominance of oxygenated species in organic aerosols in anthropogenically-influenced Northern Hemisphere midlatitudes, *Geophys. Res. Lett.*, *34*, L13801, doi:10.1029/2007GL029979.

T. S. Bates and P. K. Quinn, Pacific Marine Environmental Laboratory, NOAA, Seattle, WA 98115, USA.

D. S. Covert, Department of Atmospheric Sciences, University of Washington, Seattle, WA 98195, USA.

L. N. Hawkins and L. M. Russell, Scripps Institution of Oceanography, University of California at San Diego, La Jolla, CA 92093-0221, USA. (lmrussell@ucsd.edu)